Characterization of an Atmospheric-Pressure Helium Plasma Generated by 2.45-GHz Microwave Power

Zihao Ouyang, Vijay Surla, *Member, IEEE*, Tae Seung Cho, *Member, IEEE*, and David N. Ruzic, *Member, IEEE*

***Abstract*—An atmospheric-pressure helium plasma generated in a 2.45-GHz microwave-induced cylindrical plasma torch has been investigated. The atmospheric-pressure helium plasma can be ignited at a microwave power of less than 400 W and sustained at as low as 100 W, at a gas flow of 50 L/min. The electron temperature T_e, electron density n_e, and gas temperature T_g measured by optical emission spectroscopy are 0.28–0.5 eV, 10^{15}–10^{16} cm^{-3}, and 1000–2000 K, respectively, at a power of 200–400 W and a gas flow rate of 20–50 L/min. In addition, it is noted that $T_e \approx T_v$ (vibrational temperature) $> T_g \approx T_r$ (rotational temperature) for these experiment parameters. These results show that the helium plasma generated in this atmospheric-pressure plasma torch is in partial local thermodynamic equilibrium (pLTE).**

***Index Terms*—Atmospheric-pressure plasma, laser-assisted plasma coating at atmospheric pressure (LAPCAP), pulsed-laser ablation, pulsed-laser deposition, thermal barrier coatings.**

I. Introduction

RECENTLY, atmospheric-pressure plasma sources have been widely used for various applications due to their many advantages [1]. Depending on the discharge gases and the system configurations, a large range of the plasma gas temperatures from ambient (nonthermal) to several thousand kelvins has been demonstrated. Typical atmospheric-pressure plasmas also have large electron density ($n_e > 10^{14}$ cm^{-3}), low electron temperature (< 1 eV), and high radical concentrations. From the applications point of view, nonthermal plasma allows energetic radicals to intensively modify the substrate surfaces without thermal damage, whereas high-gas temperature plasma is favorable as heat sources for applications such as atmospheric plasma spray [2].

Atmospheric-pressure plasmas are usually considered in local thermodynamic equilibrium (LTE) due to the high collision frequency between species. However, the LTE condition cannot be applied to dc glow atmospheric-pressure plasma, owing to significant dissociation and ionization rates caused by high electron temperature T_e [3]. Therefore, several temperatures are used to describe the energy distribution: electron temperature, electronic temperature $T_{\rm el}$ (the energy for electron excitation), vibrational temperature T_v, and rotational temperature T_r. Rotational temperature is considered equivalent to gas temperature T_g because of frequent energy exchanges between plasma molecules and rotational states of these molecules due to large collision rates at high pressure [4]. In this paper, small portion of N_2 has been added to the base gas of helium to measure the gas temperature of helium plasma, which could be determined by the spectroscopic intensities of nitrogen molecules (N_2 second positive system C–B in the 300- to 420-nm range). The electron temperature has been estimated by the Boltzmann plot, assuming the ionic and atomic levels in the helium plasma satisfy the partial LTE (pLTE) condition. The electron density has been measured by the Stark broadening of H_β lines at 486.1 nm for its strong Stark broadening effect and weak self-absorption [5]. This paper provides detailed information on the behavior of an atmospheric-pressure helium plasma so that these plasma characteristics can be controlled and modified for various applications.

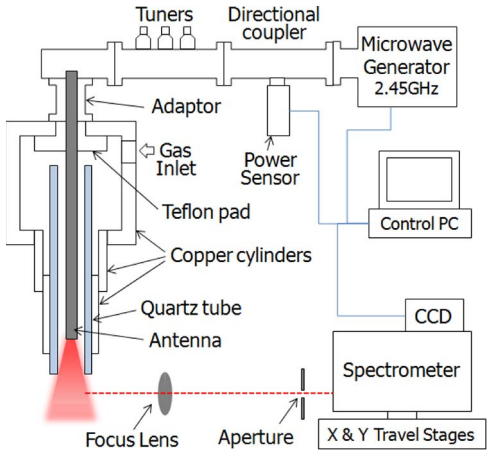

Fig. 1. Schematic of the atmospheric-pressure torch and experimental setup.

II. Experiment

The atmospheric-pressure plasma torch consists of three coaxial copper cylinders with decreasing diameters, a copper antenna at the center, and a quartz discharge tube, as shown in Fig. 1. The diameter of the antenna is 6 mm, and the discharge tube has an inside diameter of 13 mm. Gases are supplied into the atmospheric-pressure plasma torch from the gas inlet on the bottom of the outmost copper cylinder wall, and a Teflon pad is placed at the bottom of the torch to prevent arc discharge between the antenna and the copper cylinder. The atmospheric-pressure plasma has been ignited in the torch by a 2.45-GHz

Manuscript received July 30, 2012; revised September 11, 2012; accepted October 2, 2012. Date of publication November 16, 2012; date of current version December 7, 2012.

Z. Ouyang, T. S. Cho, and D. N. Ruzic are with the Center for Plasma Material Interactions, Department of Nuclear, Plasma, and Radiological Engineering, University of Illinois at Urbana-Champaign, Urbana, IL 61801 USA.

V. Surla was with the Center for Plasma Material Interactions, Department of Nuclear, Plasma, and Radiological Engineering, University of Illinois at Urbana-Champaign, Urbana, IL 61801 USA. He is now with Mattson Technology Inc., Fremont, CA 94538 USA.

Color versions of one or more of the figures in this paper are available online at http://ieeexplore.ieee.org.

Digital Object Identifier 10.1109/TPS.2012.2223238

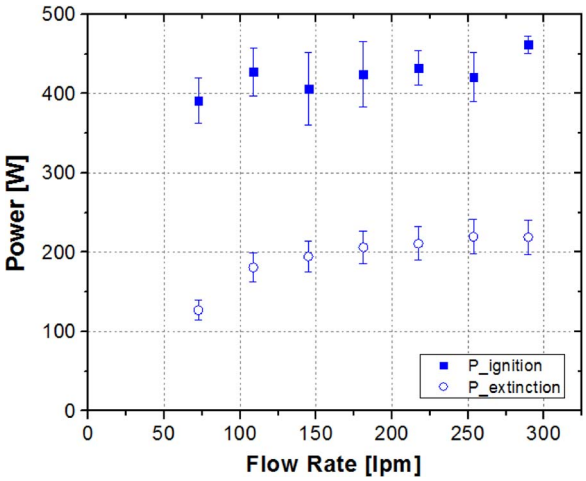

Fig. 2. Ignition and extinction powers for the atmospheric-pressure helium plasma as a function of gas flow rate.

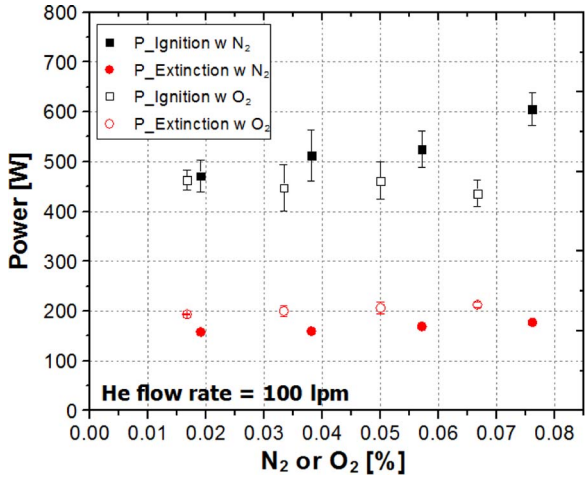

Fig. 3. Ignition and extinction powers for He–N_2 or He–O_2 plasma with a fixed helium flow rate of 100 L/min versus different mixture ratios.

microwave generator. The microwave generator has the maximum output power of 6 kW, and the reflected power was kept below 5% of input power in all experiments. Electron temperature T_e and electron density n_e have been measured by optical emission spectroscopy (OES, Acton Research Corporation, SpectraPro 275). The resolution of the OES system is 0.1 nm for 1200 g/mm.

III. Experimental Results and Discussion

A. Ignition and Extinction Powers of the Atmospheric-Pressure Plasma Torch

To study the plasma ignition and stability, the ignition and extinction powers (the lowest power to sustain the plasma) have been measured for helium alone, helium/nitrogen mixture, and helium/oxygen mixture. Fig. 2 shows the ignition and extinction powers as a function of helium flow rate. It is noted that the plasma ignites at similar power for all flow rates except 300 L/min, which needs little bit higher power. These phenomena may be originated from the high-pressure turbulence at the antenna tip. On the other hand, the extinction power increased and then saturated with increasing helium flow rate, which can be explained by the electron production–loss balance. As the flow rate is increased, the electron loss rate by the relaxation process increases due to higher collision frequency, but the electron production rate remains the same or even lower due to pressure turbulence. Thus, it requires a higher electric field to sustain the plasma.

The ignition and extinction powers can be strongly affected by adding a small proportion of other gases into the helium plasma. As shown in Fig. 3, the addition of a small amount of nitrogen to helium makes the ignition power increase from 450 to 590 W and also widens the plasma operation range. In contrast, adding oxygen decreases the plasma ignition power and increases the extinction power even more. The mechanism for the disparate behavior of the nitrogen and oxygen mixture is caused by the effect of different molecule ions, which are mostly N_2^+ and O_2^-, at these conditions. An oxygen molecule could obtain an electron and a nitrogen molecule could release an electron when they are excited; therefore, the electron production is easier to balance with the electron loss in He–N_2 plasma than in He–O_2, which results in a higher extinction power in He–O_2 plasma. Other mechanisms could also contribute to the plasma instability, for example, the instability due to the dissociative attachment between O_2^- and electrons can significantly affect the stability in an atmospheric-pressure He–O_2 plasma if the number density of O_2^- is high.

B. Plasma Gas Temperature

The N_2 second positive system ($C^3\Pi$–$B^3\Pi$) in the range of 364–383 nm has been used to determine the rotational temperature $\approx T_g$ by fitting the experimental N_2 C–B spectrum to the calculated spectrum by the SPECAIR code [6]. The variables were set the same as the previous study [7]. Generally, electronic excitation temperature $T_{\rm el}$, rotational temperature T_r, translational temperature T_t, and vibrational temperature T_v satisfy $T_{\rm el} > T_v > T_r \approx T_g \approx T_t$ for nonequilibrium plasma [8]. Each of these temperatures was independently adjusted in SPECAIR by steps of 50 K until the best fits were achieved. As an example, the best fit of the measured N_2 C–B spectrum for 400 W and 0.3 L/min of N_2 is shown in Fig. 4, which gives $T_g \approx 1800 \pm 100$ K.

Fig. 5 shows the rotational and vibrational temperatures as functions of input microwave power and N_2 flow rate. The significant differences between T_r and T_v reveals that the plasma is nonequilibrium. T_r increases from ~1000 to ~1800 K when the input power is increased from 200 to 400 W, whereas T_v has the largest value of ~5000 K at the medium power of 300 W. The cooling effect of N_2 gas flow becomes more significant at higher power and higher rotational temperature, which results in a slight decrease in T_r when the N_2 flow rate is increased.

C. Electron Temperature

Electron temperature T_e has been determined by the Boltzmann plots. The atoms, ions, and electrons were assumed to be in pLTE, and the ionization fraction was large so that there were enough free electrons to allow the density distribution of

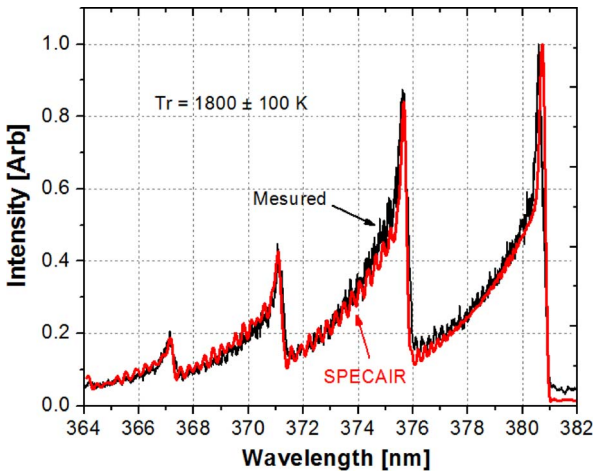

Fig. 4. Measured N_2 C–B spectrum of the helium plasma at 400 W and a N_2 flow rate of 0.3 L/min compared with the calculated spectrum using the SPECAIR code.

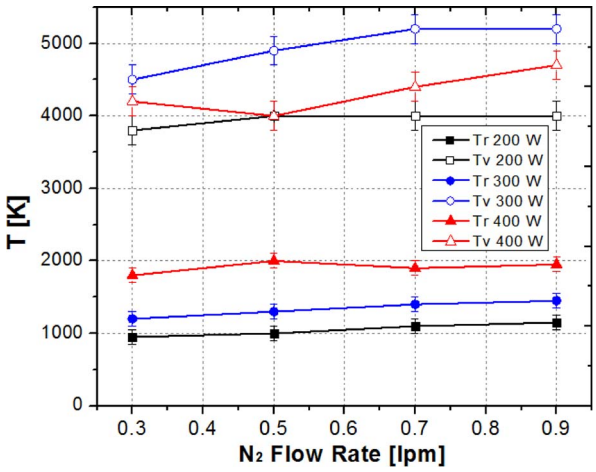

Fig. 5. Measured N_2 C–B spectrums versus input power and N_2 flow rate at a helium flow rate of 20 L/min.

excited atoms to be Boltzmann. Therefore, the relation between the spectral line intensity and the energy of an excited state satisfies [7], [9]

$$ln\frac{I_{p\to k}\lambda_{p\to k}}{g(p)A_{p\to k}} = -\frac{E(p)}{kT_e} + \text{constant} \quad (1)$$

where $I_{p\to k}$, $\lambda_{p\to k}$, and $A_{p\to k}$ are the relative intensity, peak wavelength, and Einstein constant for spontaneous emission of a specific spectral line representing a transition $p \to k$, and $g(p)$ and $E(p)$ are the statistical weights and photon energy of an excited state p, respectively. The reference data of $\lambda_{p\to k}$, $A_{p\to k}$, $g(p)$, and $E(p)$ for a particular transition can be found at NIST Atomic Spectra Database. These parameters of measured helium spectral lines are listed in Table I. Note that two or more transitions are sometimes coupled at the same wavelength, which have different $A_{p\to k}$, $g(p)$, and $E(p)$ values. The calculation for $\ln(I_{p\to k}\lambda_{p\to k}/g(p)A_{p\to k})$ of each transition was individually obtained by assuming an identical probability of each transition, and T_e was determined by the slope of the Boltzmann plot $\ln(I_{p\to k}\lambda_{p\to k}/g(p)A_{p\to k})$ versus $E(p)$.

TABLE I
TRANSITIONS SELECTED FROM THE HELIUM PLASMA IN THE PLASMA TORCH

λ/Å	$A_{p\to k}$/s^{-1}	g(p)	E(p)/cm^{-1}
3888.6480	9.4746E+06	3	185564.6
	9.4746E+06	5	185564.6
4026.1914	3.2224E+05	3	193917.2
	2.8999E+06	5	193917.2
	1.1601E+07	7	193917.2
	4.8336E+06	3	193917.2
	8.6997E+06	5	193917.2
4471.4802	6.8275E+05	3	191444.5
	6.1440E+06	5	191444.5
	2.4579E+07	7	191444.5
	1.0241E+07	3	191444.5
	1.8432E+07	5	191444.5
4713.1457	5.2894E+06	3	190298.1
	3.1736E+06	3	190298.1
4921.9313	1.9863E+07	5	191446.5
5015.6783	1.3372E+07	3	186209.4
5875.6210	1.7673E+07	5	186101.5
	7.0708E+07	7	186101.5
	2.9462E+07	3	186101.6
	5.3019E+07	5	186101.5
6678.151	6.3705E+07	5	186105.0
7065.190	1.5474E+07	3	183236.8
	9.2844E+06	3	183236.8

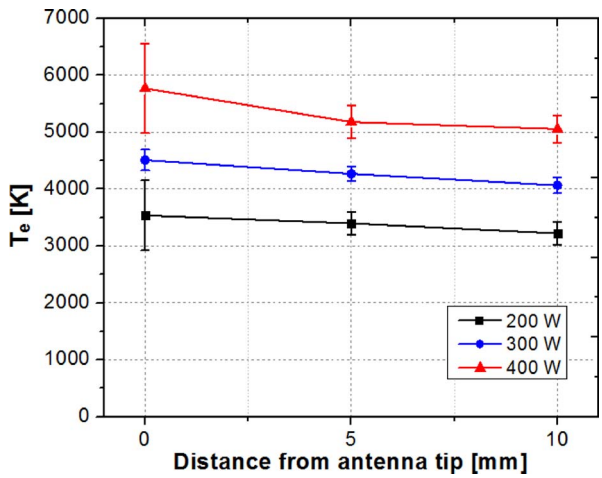

Fig. 6. Measured electron temperature as functions of input power and distance from the antenna tip at 40 L/min.

Fig. 6 shows that T_e increases from 3200 K (0.28 eV) to 5800 K (0.5 eV) when the input power is increased from 200 to 400 W, whereas its dependence on the distance from the antenna tip is not very significant within the 1-cm range downstream. This means that the helium plasma generated by the atmospheric-pressure plasma torch has spatial uniformity over a relatively large area. Fig. 7 shows T_e as a function of helium flow rate from 30 to 40 L/min. T_e seems to slightly increase as flow rate increases. The pressure at the tip of the antenna could be relatively lower and slightly decreases as the gas flow is increased. Therefore, T_e slightly increases owing to lower collision frequency with increasing flow rate. However, the error of T_e is increased at a flow rate of 50 L/min because a larger flow rate induces complexities in electron density n_e and

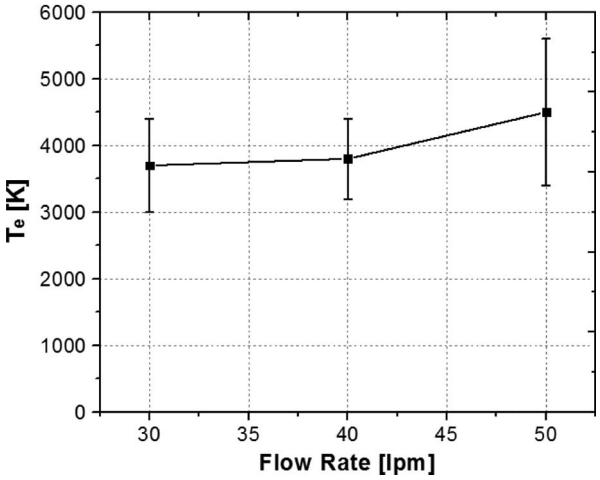

Fig. 7. Measured electron temperature versus helium gas flow rate at 200 W.

gas temperature T_g calculations by affecting the plasma cooling mechanism. Therefore, it is safer to say that T_e does not have very strong dependence on the helium flow rate.

D. Electron Density

Electron density n_e is calculated from the full-width at half-maximum (FWHM) of the atomic hydrogen spectrum due to Stark broadening. The H_β spectral line at 486.1 nm is chosen for measuring the electron density for its strong Stark broadening effect and weak self-absorption [5], [10], i.e.,

$$\Delta\lambda_{\text{Stark}} = 2.50 \times 10^{-9} \alpha_{1/2} n_e^{2/3} \tag{2}$$

where $\Delta\lambda_{\text{Stark}}$ is in nanometers, n_e is in per cubic centimeter, and $\alpha_{1/2}$ is the reduced wavelength tabulated by Griem [11]. For the H_β line, $\alpha_{1/2}$ is typically from 7.62×10^{-3} to 8.03×10^{-3} nm for T_e in the range of 5000–10 000 K and n_e in the range of 10^{14}–10^{15} cm^{-3}. $\alpha_{1/2} = 7.83 \times 10^{-3}$ nm is used as an average value in this paper. Less than 1% hydrogen was introduced into the plasma in order to obtain a strong spectral signal to improve the experimental accuracy without significant perturbation of plasma dynamics.

Three major broadening mechanisms, namely, instrumental broadening, Doppler broadening, and Van der Waals broadening, contribute to the overall line shape, in addition to Stark broadening. Other broadening mechanisms, such as resonance broadening [11], [12], are assumed to be relatively insignificant due to the fact that the fraction of hydrogen atoms is small enough. Each of these broadening mechanisms is considered either Gaussian shape (such as instrumental broadening and Doppler broadening) or Lorentzian shape (such as Stark broadening and Van der Waals broadening). The resulting overall convolution line shape is a Voigt profile. Each of these broadening mechanisms is determined by the following methods: 1) *Instrumental broadening.* The diffraction dispersion that resulted from the slit opening of the OES system leads to broadening in all spectral lines. In this paper, it is represented by the FWHM of a He–Ne laser spectral line at 632.8 nm. 2) *Doppler broadening.* If the velocity distribution of the hydrogen atoms can be approximated by a Maxwell–Boltzmann function in pLTE plasma, Doppler broadening is estimated by

TABLE II
FWHM (IN NANOMETERS) OF DIFFERENT BROADENING MECHANISMS FOR THE H_β LINE AT 486.1 nm

$\Delta\lambda_{instrument}$	$\Delta\lambda_D$	$\Delta\lambda_\alpha$	$\Delta\lambda_{Stark}$
0.193	$1.72 \times 10^{-4} T_g^{1/2}$	$1.9 T_g^{-0.7}$	$1.96 \times 10^{-11} n_e^{2/3}$

$$\Delta\lambda_D = \lambda_0 \left(\frac{8kT_g ln2}{mc^2}\right)^{1/2} = 7.16 \times 10^{-7} \lambda_0 \left(\frac{T_g}{M}\right)^{1/2} \tag{3}$$

where $\lambda_0 = 486.1$ nm is the central wavelength of the H_β line; T_g is the gas temperature of the plasma in kelvins; and m and M are the atomic mass of the emitter (He atom) in kilograms and atomic mass units, respectively. 3) *Van der Waals broadening.* This broadening mechanism is originated from the dipolar interaction between the excited atoms (the emitter) with the dipoles formed by the excited atoms and a neutral molecule in the ground state (the perturber). The half-width at half-maximum of the Van der Waals broadening in the frequency space is given by [12]

$$\Delta\omega_\alpha = \pi N \left(\frac{9\pi\hbar^5 \overline{R_\alpha^2}}{16 m_e^3 E_p^2}\right)^{\frac{2}{5}} \overline{\nu^{\frac{3}{5}}} \tag{4}$$

where $N = P/kT_g$ is the number density of the perturber, and v is the relative speed of the emitter and the perturber, which is related to the mean speed of the atoms, i.e.,

$$\overline{\nu^{\frac{3}{5}}} = \left(\frac{4}{\pi}\right)^{\frac{2}{10}} \Gamma\left(\frac{9}{5}\right) (\overline{v})^{\frac{3}{5}} = 0.98 \left(\frac{8kT_(g)}{\pi\mu}\right)^{\frac{3}{10}} \tag{5}$$

μ is the reduced mass of the emitter–perturber pair, $\overline{R_\alpha^2}$ is the matrix element, and E_p is the energy of the first excited state of the perturber. In a helium plasma, $E_g = 24.6$ eV, and $\overline{R_\alpha^2} \approx 520$ for the H_β line [6]. Therefore, the FWHM of the Van der Waals broadening in this paper can be written as

$$\Delta\lambda\alpha = 0.98 \frac{\lambda_0^2}{c} \frac{P}{kT_g} \left(\frac{9\pi\hbar^5 \overline{R_\alpha^2}}{16 m_e^3 E_p^2}\right)^{\frac{2}{5}} \left(\frac{8kT_g}{\pi\mu}\right)^{\frac{3}{10}} = \frac{1.9}{T_g^{0.7}} \tag{6}$$

where $\Delta\lambda_\alpha$ is in nanometers, and T_g is in kelvins. The helium plasma has a smaller Van der Waals broadening effect compared with air or argon plasmas due to large E_p. Table II lists the expressions for these broadening mechanisms.

The FWHM of a Voigt line shape with Gaussian width w_G and Lorentzian width w_L is empirically given by [13]

$$\Delta\lambda_{\text{Voigt}} = 0.5346 \Delta w_L + 10 \left[0.2166 (\Delta w_L)^2 + 1.3862 (\Delta w_G)^2\right]^{\frac{1}{2}}. \tag{7}$$

Therefore, Stark broadening can be expressed by

$$\Delta\lambda_{\text{Stark}} = \Delta\lambda_{\text{Voigt}} - \sqrt{(\Delta\lambda_{\text{instrument}})^2 + (\Delta\lambda_D)^2} - \Delta\lambda_\alpha. \tag{8}$$

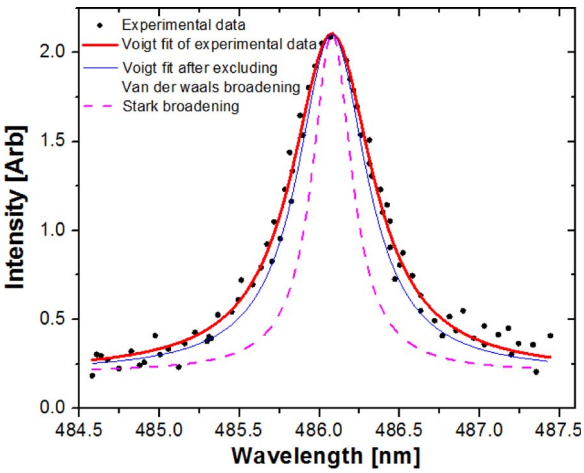

Fig. 8. H_β line shape at an input power of 200 W and a helium flow rate of 50 L/min. The spectrum is taken 10 mm away from the tip of the antenna. (Thick red line) Voigt fit of the experimental data. (Thin blue line) Fit after excluding Van der Waals broadening. (Dashed magenta) Fit after excluding the instrumental, Doppler, and Van der Waals broadening mechanisms, which is estimated to be the line shape of Stark broadening.

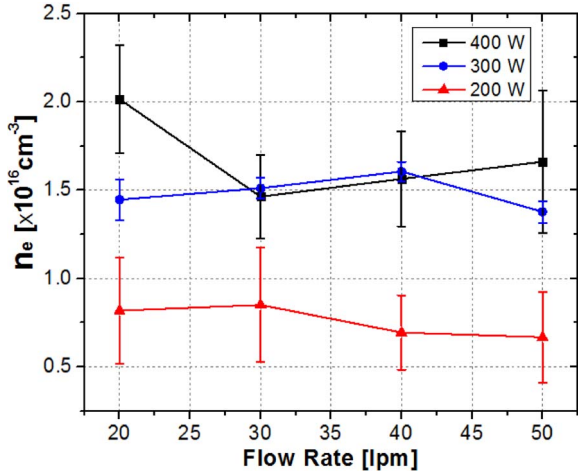

Fig. 9. n_e of the helium plasma as functions of input power and helium flow rate at the tip of the antenna.

The profile of the H_β line (200 W, 50 L/min He) is shown in Fig. 8. The Stark broadening line shape is obtained after excluding the Van der Waals and Gaussian broadening mechanisms from the measured spectrum. Fig. 9 shows the behavior of n_e as a function of the input power and gas flow rate. The calculations show that n_e values are in the range of 10^{15}–10^{16} cm^{-3} when the input power is increased from 200 to 400 W. Although n_e significantly increases from 200 to 300 W, it does not change as much when the input power is further increased to 400 W. This may result from the electron loss during the occasional arcing process between the antenna and the inside wall of the plasma torch at high input powers. It is also shown in Fig. 9 that n_e does not have strong dependence on the helium flow rate.

IV. Conclusion

A 13-mm-diameter helium plasma has been generated by the atmospheric-pressure plasma torch and sustained at an input power as low as 100 W. A detailed analysis has been presented for measuring the electron temperature T_e, electron density n_e, and gas temperature T_g of a helium plasma. The Boltzmann plots gives a T_e in the range of 3200–5800 K when the input power is increased from 200 to 400 W, but its dependence on the distance from the antenna tip is not significant. Rotational temperature T_r is assumed to be equal to T_g, which gives a T_g of 1000–2000 K when the power is increased from 200 to 400 W. However, T_v has a value close to T_e in the power range of 200–400 W. From these results ($T_e \approx T_v > T_r$), it is obvious that the atmospheric-pressure helium plasma is not in thermal equilibrium and could be considered in pLTE. Electron density n_e has been calculated from the Stark broadening of the H_β line, which is in the range of 10^{15}–10^{16}cm^{-3} for the input power of 200–400 W.

References

[1] M. Moisan, J. Hubert, J. Margot, G. Sauve, and Z. Zakrzewski, *Microwave Discharges: Fundamentals and Applications*, C. M. Ferreira and M. Moisan, Eds. New York: Plenum, 1993.
[2] L. Pawlowski, *The Science and Engineering of Thermal Spray Coatings*, 2nd ed. Chichester, U.K.: Wiley, 2008.
[3] L. Yu, D. M. Packan, C. O. Laux, and C. H. Kruger, "Direct-current glow discharges in atmospheric pressure air plasmas," *J. Appl. Phys.*, vol. 91, no. 5, pp. 2678–2686, Mar. 2002.
[4] R. M. Clements, C. S. MacLatchy, and P. R. Smy, "Verification of static spherical probe theory in a moving high-pressure plasma," *J. Appl. Phys.*, vol. 43, no. 1, pp. 31–37, Jan. 1972.
[5] J. M. Luque, M. D. Calzada, and M. Saez, "Experimental research into the influence of ion dynamics when measuring the electron density from the Stark broadening of the H_α and H_β lines," *J. Phys. B, At. Mol. Opt. Phys.*, vol. 36, no. 8, pp. 1573–1584, Apr. 2003.
[6] C. O. Laux, "Radiation and nonequilibrium collisional-radiative models," in *Physico-Chemical Modeling of High Enthalpy and Plasma Flows*, D. Fletcher, J-M. Charbonnier, G. R. Sarma, and T. Magin, Eds. Rhode-Saint-Genèse, Belgium: Von Karman Inst., 2002, Lecture Series.
[7] Z. Ouyang, L. Meng, P. Raman, T. S. Cho, and D. N. Ruzic, "Laser-assisted plasma coating at atmospheric pressure: Production of yttria-stabilized zirconia thermal barriers," *J. Phys. D, Appl. Phys.*, vol. 44, no. 26, p. 265 202, Jul. 2011.
[8] D. Staack, B. Farouk, A. Gutsol, and A. Fridman, "Characterization of a DC atmospheric pressure normal glow discharge," *Plasma Sources Sci. Technol.*, vol. 14, no. 4, pp. 700–711, Nov. 2005.
[9] A. Gamero, "Spectroscopic diagnostics of high pressure discharges," *J. Phys. IV France*, vol. 8, no. PR7, pp. Pr7-339–Pr7-348, Oct. 1998.
[10] H. R. Griem, *Plasma Spectroscopy*. New York: McGraw-Hill, 1964.
[11] H. R. Griem, *Spectral Line Broadening by Plasmas*. New York: Academic, 1974.
[12] C. O. Laux, T. G. Spence, C. H. Kruger, and R. N. Zare, "Optical diagnostics of atmospheric pressure air plasmas," *Plasma Sources Sci. Technol.*, vol. 12, no. 2, pp. 125–128, May 2003.
[13] J. J. Olivero and R. L. Longbothum, "Empirical fits to the Voigt line width: A brief review," *J. Quantitative Spectr. Radiative Transf.*, vol. 17, no. 2, pp. 233–236, Feb. 1977.

Zihao Ouyang received the B.S. degree in physics from Peking University, Beijing, China, in 2008 and the M.S. degree in nuclear, plasma, and radiological engineering from the University of Illinois at Urbana-Champaign in 2011. He is currently working toward the Ph.D. degree at the University of Illinois at Urbana-Champaign.

From 2008 to 2011, his primary research interests are atmospheric-pressure plasma sources, plasma modeling and diagnostics, and pulsed-laser deposition applications. Since 2011, he has been working on developing dry-etch methods for noble metals and optimizing dry-etch processes for through-silicon vias.

Vijay Surla (M'10) received Ph.D. degree in mechanical engineering from Colorado State University, Fort Collins, in 2007.

He was a Postdoctoral Research Associate with the Zarelab, Stanford University, Stanford, CA, in 2007–2008 and with the Center for Plasma Material Interactions (CPMI), Department of Nuclear, Plasma, and Radiological Engineering, University of Illinois at Urbana-Champaign, in 2008–2010. From 2010 to 2011, he continued to work at CPMI as a Research Engineer and visited Princeton Plasma Physics Laboratory as a collaborator to study edge plasma interactions in the National Spherical Tokamak Experiment. He is currently a Senior Product Engineer with Mattson Technology Inc., Fremont, CA, working on the development of next-generation plasma sources for semiconductor processing. Throughout his career, he has gained extensive experience in developing diagnostics for various types of plasma applications. His current research interests include fundamental and applied aspects of plasmas and plasma–material interactions for applications in fusion energy, material processing, and high-value manufacturing.

Tae Seung Cho (M'08) received the B.S., M.S., and Ph.D. degrees from Kwangwoon University, Seoul, Korea, in 1995, 1998, and 2002, respectively.

From 2002 to 2003, he was a Research Scholar with the Stevens Institute of Technology, Hoboken, NJ, where he worked on the applications of dielectric barrier discharge and capillary discharge. From 2003 to 2005, he was a Senior Engineer with Plasmion Corporation, Hoboken, where his research concern was the capillary plasma application for surface modification and flat-panel display. From 2005 to 2010, he was with the R&D Center and PDP Development Team, Samsung SDI Company, Ltd., Cheonan, Korea, as a Senior Engineer. He is currently a Research Scholar with the Center for Plasma Material Interactions, Department of Nuclear, Plasma, and Radiological Engineering, University of Illinois at Urbana-Champaign. His current research fields are in plasma diagnostics, microplasma applications, dielectric barrier discharge, atmospheric plasma application, and plasma processing for microelectronics industry.

David N. Ruzic (M'01) received the Ph.D. degree in physics from Princeton University, Princeton, NJ, in 1984.

He is the Director of the Center for Plasma Material Interactions, Department of Nuclear, Plasma, and Radiological Engineering, University of Illinois at Urbana-Champaign. He is a Professor with the Department of Nuclear, Plasma, and Radiological Engineering and affiliated with the Department of Electrical and Computer Engineering and the Department of Physics, having joined the faculty in 1984. His current research interests center on plasma processing for the microelectronics industry (deposition, etching, extreme ultraviolet lithography, and particle removal), atmospheric-pressure plasmas for industrial applications, and fusion energy research. He has a passion for teaching, particularly about energy sources, because he gets to blow something up in almost every class.

Dr. Ruzic is a Fellow of the American Nuclear Society and the American Vacuum Society.